RSC Advances

PAPER

View Article Online
View Journal | View Issue

Cite this: *RSC Adv.*, 2017, **7**, 23127

Fluorescent detection of multiple ions by two related chemosensors: structural elucidations and logic gate applications†

Vijay Kumar,‡ Pramod Kumar‡ and Rajeev Gupta *

Received 4th February 2017
Accepted 18th April 2017

DOI: 10.1039/c7ra01453h

rsc.li/rsc-advances

Two related chemosensors L1 and L2 display selective detection of multiple ions (Cu^{2+}, Al^{3+}, Cd^{2+} and S^{2-}) as a result of minor variation of functional groups. Both chemosensors offer identical pyrrole-2-carboxamide fragments; however, they differ by the presence of either an ester (L1) or an acid group (L2) at a remote arene ring. While L1 shows selectivity towards the Cu^{2+} ion L2 is highly selective for Al^{3+} and Cd^{2+} cations as well as S^{2-} anion. A combination of studies (Stern–Volmer plots, detection limits and Benesi–Hildebrand fittings) displays the notable sensing abilities of both chemosensors. Both chemosensors were utilized to develop logic gate-based applications by considering multiple detection of assorted ions. Structural studies provide vital details about the mode of binding between chemosensors and cations. Simple synthesis, multi-stimuli response, fast response, solution visualization, and practical detection methods (filter paper strips and polystyrene films) suggest excellent sensing potentials of both chemosensors.

Introduction

Development of strategies for the detection of multiple ions has received considerable attention due to significance in biological, environment, and chemical assays.[1] Detection of multiple ions by a single probe is not only cost-effective and time-saving but is also desirable for one-pot assays.[2] Moreover, probes capable of detecting multiple ions have been effectively used for the development of memory devices and molecular logic gates.[3] In this direction, molecular logic gates with proper input and output history are appropriate for such memory devices.[4] However, progress is still in its infancy and hence multiple inputs/outputs based logic operations are required with better safety level and multiple inputs.[5] Notably, inputs and outputs critically depend on the functional groups being offered by a probe and/or a chemosensor.[6]

It is well known that both cations and anions are required in various biological processes while both their excess as well as deficiency may have detrimental effects.[7] For example, essential Cu^{2+} ion can cause serious complications due to its excess.[8,9] Accumulation of aluminum induces several health hazards such as Alzheimer's and Parkinson's diseases while it can also damage the nervous system.[10] Contamination of cadmium in environment causes serious environmental and health problems, including lung, prostatic, and renal cancers.[11] Similarly, high level of several anions such as sulfide can cause irritation of mucous membrane, and may lead to unconsciousness and respiratory paralysis, Alzheimer's disease, Down's syndrome and liver cirrhosis.[12,13] Therefore, detection of several such cations and anions is important due to their momentous effect both on human health and environment.[14,15]

Synthetic chemosensors have been developed for the individual detection of Cu^{2+},[16,17] Al^{3+},[18] Cd^{2+},[19] and S^{2-} ions.[20,21] However, detection of multiple ions by a single chemosensor has been a major challenge.[22–24] Martinez-Manez and co-workers have reported detection of multiple ions based on a single chemosensor in its different forms.[25] On the other hand, Schmittel and co-workers have achieved technique-dependent selective detection of multiple ions.[26] However,

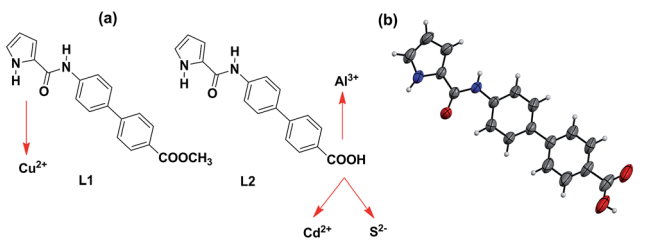

Scheme 1 (a) Chemical drawings of chemosensors L1 and L2 and their mode of interaction with multiple ions; (b) molecular structure of chemosensor L2 wherein thermal ellipsoids are drawn at 50% probability level.

Department of Chemistry, University of Delhi, Delhi 110 007, India. E-mail: rgupta@chemistry.du.ac.in; Web: http://www.people.du.ac.in/~rgupta/; Tel: +91-11-27666646

† Electronic supplementary information (ESI) available: Experimental details for the determination of Stern–Volmer constants, detection limits and binding constants; and X-ray crystallography; figures for FTIR, NMR, mass, absorption, and emission spectra, binding constants, detection limit, optical images, and a table for X-ray data collection. CCDC 1530941 and 1530943. For ESI and crystallographic data in CIF or other electronic format see DOI: 10.1039/c7ra01453h

‡ These authors contributed equally to this work.

development of a single chemosensor, capable of detecting multiple ions, still remains a difficult task. Herein, we present two closely related chemosensors L1 and L2 with adept detection abilities for multiple ions (Cu^{2+}, Al^{3+}, Cd^{2+} and S^{2-}). These chemosensors include biphenyl moiety as the fluorophore while pyrrole-2-carboxamide and carboxylic acid groups serve as the ion interacting sites (Scheme 1).

Results and discussion

Synthesis and characterization of L1 and L2

Chemosensor L1 was synthesized by the coupling of pyrrole-2-carboxylic acid with methyl-4-amino-[1,1-biphenyl]-4-carboxylate whereas L2 was obtained by the base-assisted hydrolysis of L1. FTIR spectrum shows two N–H stretches at 3405 and 3326 cm^{-1} for L1 and 3334 and 3284 cm^{-1} for L2 (Fig. S1 and S2, ESI†). Such stretches have been assigned to the presence of pyrrole-NH and amide-NH resonances.[27] Similarly, proton NMR spectrum of L1 displays two signals for two different N–H groups at 9.82 and 11.69 ppm. On the other hand, L2 exhibits two such signals at 9.85 and 11.67 ppm whereas a broad feature at 12.90 ppm corresponds to –COOH group (Fig. S3–S6, ESI†). The ESI^+ mass spectra of chemosensors L1 and L2 display $[L + H]^+$ molecular ion peaks at 321.1237 and 307.1079, respectively (Fig. S7 and S8, ESI†). Chemosensor L2 crystallized in $P2_1/c$ space group and its molecular structure is shown in Scheme 1b. The crystal structure displays that the biphenyl and pyrrole rings exist in the same plane while pyrrole-N and carboxamide-O groups are nicely positioned on the same side to potentially chelate a metal ion.

Detection of Cu^{2+}, Al^{3+}, Cd^{2+} and S^{2-} ions

The UV-Vis spectra of chemosensors L1 and L2 in CH_3OH display intense peaks at 312 nm (44 240 mol^{-1} cm^{-1}) and 307 nm (41 050 mol^{-1} cm^{-1}) (Fig. S9, ESI†). Such features are assigned to π–π^* transitions within these chemosensors. Both

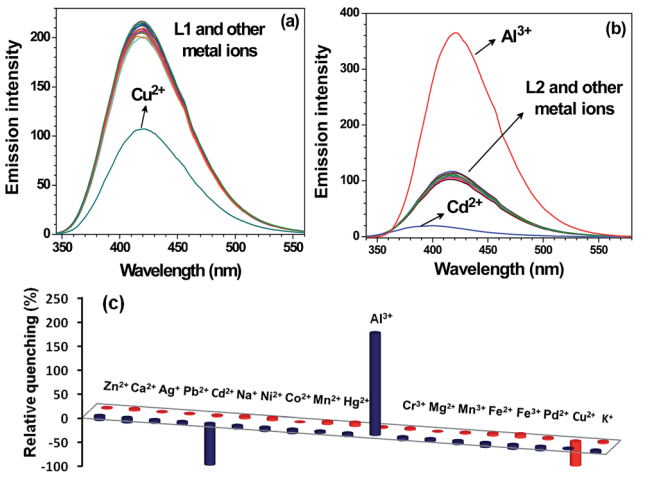

Fig. 1 Emission spectra of chemosensor (a) L1 (20 μM) and (b) L2 (20 μM) in CH_3OH and after their interaction with assorted metal ions (100 μM). Bar diagram exhibiting change in emission intensity at 418 nm for L1 (red pillars) and L2 (blue pillars) in presence of assorted metal ions (100 μM).

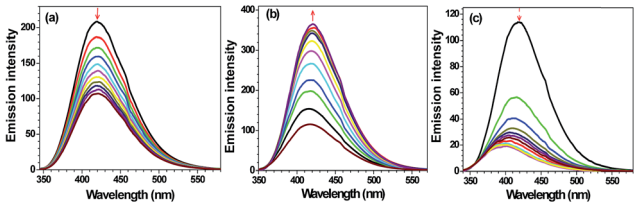

Fig. 2 Change in emission intensity in CH_3OH of (a) L1 (20 μM) on exposure to Cu^{2+} ion (0–100 μM); (b) and (c) L2 (20 μM) on exposure to Al^{3+} and Cd^{2+} ions (0–100 μM), respectively.

L1 and L2 show intense emission at 418 nm upon excitation at 320 nm in CH_3OH. We evaluated the effect of addition of alkali (Na^+, K^+), alkaline (Mg^{2+}, Ca^{2+}), transition (Cr^{3+}, Co^{2+}, Ni^{2+}, Fe^{2+}, Fe^{3+}, Mn^{2+}, Mn^{3+}, Cu^{2+}, Zn^{2+}, Ag^+, Hg^{2+}, Pd^{2+}, Cd^{2+}) and post-transition (Al^{3+}, Pb^{2+}) metal ions on the emission spectra of L1 and L2. Notably, addition of five equivalents (100 μM) of assorted metal ions to L1 (20 μM) did not cause appreciable change. However, addition of Cu^{2+} ion resulted in considerable quenching in the emission intensity when compared to other metal ions (Fig. 1). Interestingly, in case of L2, Al^{3+} triggers enhancement with moderate red shift ($\Delta\lambda = 3$ nm) whereas Cd^{2+} caused notable quenching in the emission with considerable blue shift ($\Delta\lambda = 25$ nm) (Fig. 1).

As probe L2 showed emission enhancement in presence of Al^{3+} ion, hence, we measured the fluorescence spectra of L2 in absence as well as in presence of Al^{3+} ion in different combinations of CH_3OH and H_2O (CH_3OH/H_2O; 100 : 0, 75 : 25, 50 : 50, 25 : 75, 10 : 90, 1 : 99). Fig. S10† shows that increasing water percentage quenches the emission of L2. Similarly, detection of Al^{3+} ion by chemosensor L2 was also higher in CH_3OH when compared to a MeOH–H_2O mixture (Fig. S11†). In light of these observations, sensing studies were only performed in CH_3OH and not in 100% H_2O or HEPES buffer.

The change in the fluorescence intensity of L1 and L2 was investigated by the successive addition of Cu^{2+}, Al^{3+} and Cd^{2+} ions (Fig. 2 and 3a). Importantly, Cu^{2+} ion shows quenching without wavelength shift whereas Al^{3+} and Cd^{2+} ions respectively exhibited enhancement and quenching with wavelength shift. To measure the extent of binding, Stern–Volmer constants (K_{SV}),[28] detection limits[29] and binding constants (K_b)[30] were calculated using fluorescence spectral titrations. The Stern–Volmer constants were found to be 9.33×10^3 M^{-1} and 5.95×10^4 M^{-1} for Cu^{2+} and Cd^{2+} ions, respectively (Fig. S12† and Table 1). Chemosensor L1 showed the detection limit of 1.39 μM for Cu^{2+} ion while L2 showed detection limits of 0.55 μM and 1.02 μM for Al^{3+} and Cd^{2+} ions, respectively (Fig. S13† and Table 1). The binding constants K_b (M^{-1}) were found to be 1.61×10^4, 3.72×10^3 and 1.24×10^5 for Cu^{2+}, Al^{3+} and Cd^{2+} ions, respectively (Fig. 3b and Table 1).[30]

The detection of Cu^{2+}, Al^{3+} and Cd^{2+} ions by the photo-responsive chemosensors L1 and L2 was also investigated by the UV-Vis spectral titrations. The intense peak at λ_{max} = 312 nm (44 240 mol^{-1} cm^{-1}) for L1 (20 μM, CH_3OH) was red-shifted by 4 nm in presence of Cu^{2+} ion (0–100 μM). The observation of two isosbestic points at 288 and 330 nm suggests

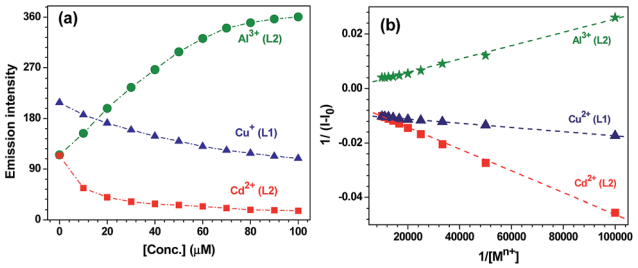

Fig. 3 (a) Change in emission intensity of L1 (20 μM) and L2 (20 μM) at 418 nm with varying concentration of Cu^{2+}, Al^{3+} and Cd^{2+} ions (100 μM). (b) Benesi–Hildbrand plots at 418 nm for Cu^{2+}, Al^{3+} and Cd^{2+} ions with L1 and L2.

Table 1 Stern–Volmer constants (K_{SV}), detection limits and binding constants (K_b) for chemosensors L1 and L2 with Cu^{2+}, Al^{3+}, Cd^{2+} and S^{2-} ions

Species	K_{SV} (M^{-1})	Detection limit (μM)	K_b (M^{-1})	
			Fluorescence	UV-visible
L1 + Cu^{2+}	9.33×10^3	1.39	1.61×10^4	0.77×10^3
L2 + Al^{3+}	—	0.55	3.72×10^3	1.01×10^4
L2 + Cd^{2+}	5.95×10^4	1.02	1.24×10^5	0.73×10^4
L2 + S^{2-}	4.21×10^6	0.01657	1.25×10^6	1.49×10^4

the formation of a new species (Fig. 4a). Chemosensor L2 (20 μM, CH_3OH) displays an intense peak at $\lambda_{max} = 307$ nm (41 050 mol^{-1} cm^{-1}) which was red-shifted to 317 nm ($\Delta\lambda = 12$ nm) on addition of Al^{3+} ion (0–100 μM). The isosbestic points at 260 nm and 313 nm point towards the generation of a new species (Fig. 4b). The switch-on behavior of chemosensor L2 in presence of Al^{3+} ion was clearly noted under the UV light (Fig. 4b, inset). Similarly, chemosensor L2 (20 μM, CH_3OH) showed a red shift of 5 nm on addition of Cd^{2+} ion (0–100 μM) with isosbestic points at 250 nm and 310 nm (Fig. S14†). Benesi–Hildebrand fitting of UV-visible spectral titrations provided the binding constants ($K_b \times 10^3$ M^{-1}) of 0.77, 10.1 and 7.3 for Cu^{2+}, Al^{3+} and Cd^{2+} ions, respectively (Fig. S15† and Table 1).[31]

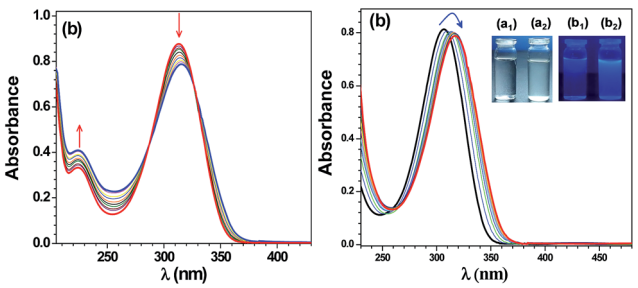

Fig. 4 (a) Change in absorption spectra of chemosensor L1 (20 μM) after addition of different concentrations of Cu^{2+} ion (0–100 μM). (b) Change in absorption spectra of chemosensor L2 (20 μM) with Al^{3+} ion (0–100 μM); inset: color change of a CH_3OH solution of L2 in absence (a_1, b_1) and in presence of Al^{3+} ion (a_2, b_2) under visible and UV light, respectively.

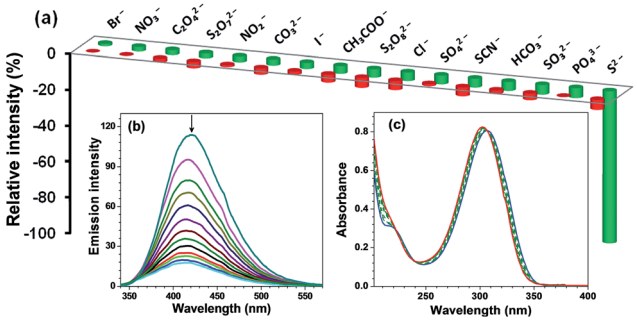

Fig. 5 (a) Bar diagram exhibiting change in emission intensity in CH_3OH at 418 nm of chemosensors L1 (20 μM, red pillars) and L2 (20 μM, green pillars) in presence of 1.2 equivalents of different anions (24 μM). (b) Change in emission spectra of L2 (20 μM) on exposure to S^{2-} ion (0–24 μM) in CH_3OH. (c) Change in absorption spectra of chemosensor L2 (20 μM) with different concentrations of S^{2-} ion (0–30 μM).

The presence of N–H groups both from pyrrole and amide moieties suggested that chemosensors L1 and L2 may also offer anion sensing abilities. Therefore, we investigated the effect of following anions on the emission of L1 and L2: SCN^-, SO_4^{2-}, SO_3^{2-}, S^{2-}, $S_2O_8^{2-}$, $S_2O_7^{2-}$, $C_2O_4^{2-}$, CH_3COO^-, CO_3^-, HCO_3^-, Cl^-, Br^-, I^-, NO_3^-, NO_2^- and PO_4^{3-}. In case of L1 (20 μM), addition of 1.2 equivalents (24 μM) of any anion did not cause appreciable change. Importantly, in case of L2 (20 μM), addition of S^{2-} ion resulted in significant quenching in the emission spectrum with a blue shift ($\Delta\lambda = 7$ nm) (Fig. S16† and 5a). The change in fluorescence intensity of L2 was then investigated by the successive addition of S^{2-} ion (Fig. 5b and S17a†). The Stern–Volmer constant (K_{SV})[28] was found to be 4.21×10^6 M^{-1} suggesting a strong quenching by S^{2-} ion (Fig. S17b† and Table 1).[32] A high detection limit of 16.57 nM and a high binding constant (K_b, M^{-1}) of 1.25×10^6 were observed for S^{2-} ion.[29,30] (Fig. S18† and Table 1). Detection of S^{2-} ion by chemosensor L2 was also investigated by the UV-visible titration in CH_3OH. The intense peak at 307 nm (20 μM) was found to blue shift ($\Delta\lambda = 4$ nm) after the addition of S^{2-} ion (0–30 μM) (Fig. 5c). Benesi–Hildebrand fitting of the UV-visible spectral titration data provided K_b of 1.49×10^4 M^{-1} (Fig. S19† and Table 1).

Selectivity studies

A good chemosensor should not only offer high sensitivity and fast response time but also high degree of selectivity for an analyte from a mixture. Therefore, selectivity was investigated by performing competitive binding studies of L1 towards Cu^{2+} and L2 towards Al^{3+} as well as Cd^{2+} ion in presence of other ions. As shown in Fig. 6a, no significant change in the emission intensity of chemosensor L1 (20 μM) towards Cu^{2+} ion was observed in presence of following metal ions (100 μM): Na^+, K^+, Mg^{2+}, Ca^{2+}, Al^{3+}, Cr^{3+}, Co^{2+}, Fe^{2+}, Fe^{3+}, Mn^{2+}, Ni^{2+}, Mn^{3+}, Zn^{2+}, Ag^+, Pb^{2+}, Hg^{2+}, Pd^{2+}, Cd^{2+}. Similarly, no remarkable change in the emission intensity of L2 (20 μM) in presence of Al^{3+} ion was observed upon addition of (100 μM) of other metal ions. As expected, however, Cd^{2+} ion showed considerable quenching (Fig. 6b). The selectivity was also investigated for S^{2-} ion in

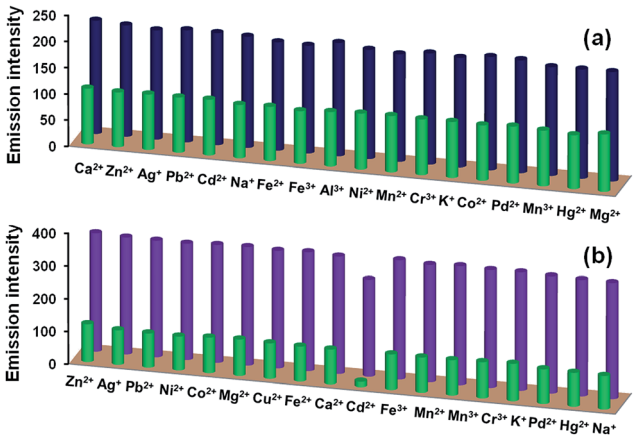

Fig. 6 (a) Selectivity of chemosensor L1 towards Cu^{2+} ion in presence of other metal ions: L1 + metal ions (blue pillars); and L1 + metal ions + Cu^{2+} ion (green pillars). (b) Selectivity of chemosensor L2 towards Al^{3+} ion in presence of other metal ions: L2 + metal ions (green pillars); and L2 + metal ions + Al^{3+} ion (purple pillars).

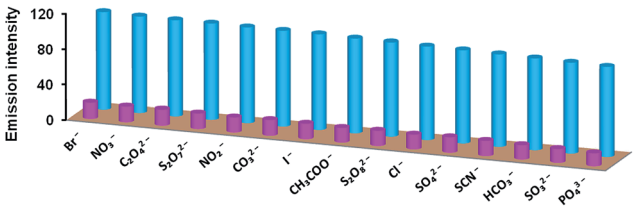

Fig. 7 Selectivity of chemosensor L2 towards S^{2-} ion in presence of other anions: L2 + anions (blue pillars); and L2 + anions + S^{2-} ion (pink pillars).

presence of other potential anions by performing competitive binding studies as shown in Fig. 7. In this case also, addition of other interfering anions (24 μM) only caused negligible change in the emission intensity of chemosensor L2 (20 μM).

Interestingly, in presence of both Al^{3+} and Cd^{2+} ions, emission intensity of chemosensor L2 was found to enhance, hence Al^{3+} ion is more dominating as compared to Cd^{2+} ion (Fig. 8, green bars). Similarly, for a combination of Al^{3+} and S^{2-} ions, Al^{3+} ion is more dominating as compared to S^{2-} ion and enhances the emission intensity of L2 (Fig. 8, blue bars). Therefore, high degree of selectivity of probe L2 towards Al^{3+} ion as compared to Cd^{2+} and S^{2-} ions, was used for the construction of two-input combinational logic circuit.[3,4,33,34] The logic circuit and the corresponding truth table was planned in such a way that Al^{3+} acts as IN 1 while Cd^{2+}/S^{2-} function as the IN 2. The change in emission intensity of L2 at 418 nm was selected as the output with the threshold value of 200 (Fig. 8). The emission above the threshold values is assigned as "ON" whereas emission below the threshold values was allocated as "OFF" for "on" and "off" readout signals, respectively. Fig. 8 displays the simplest symbolic representation of a TRANSFER (Al^{3+}) logic gate in which Al^{3+} line goes into a YES gate[35] whereas Cd^{2+}/S^{2-} line is left unconnected. Herein, YES gate output is the fluorescence intensity at 418 nm.

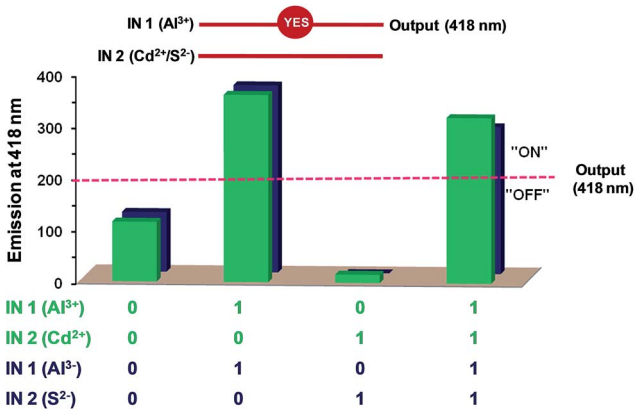

Fig. 8 Emission outputs of L2 at 418 nm in presence of chemical inputs *viz.* IN 1 = Al^{3+} and IN 2 = Cd^{2+} (green bars); IN 1 = Al^{3+} and IN 2 = S^{2-} (blue bars) and the corresponding two-input combinational logic circuit; dotted line provides guide to eyes.

Reversibility studies

Reversibility is an important factor for the optimum functioning of a chemosensor.[36] In case of Cu^{2+} ion, Na_2S was used to remove Cu^{2+} ion to achieve the reversibility.[37] Fig. 9a shows that Cu^{2+} ion quenches the fluorescence of L1; however, addition of sulfide ion restores it (*ca.* 96%). Reversibility cycles were generated for L1 (20 μM) at 418 nm upon successive addition of Cu^{2+} (100 μM) and S^{2-} (200 μM) ions (Fig. 9b). Similarly, in order to develop a reversible chemosensor for the detection of Al^{3+} and Cd^{2+} ions, K_2HPO_4 was used to remove Al^{3+} (red bars) as well as Cd^{2+} ions (green bars) from L2–Al and L2–Cd systems (Fig. 10a). Reversibility cycles were generated for L2 (20 μM) by the successive addition of Al^{3+}/Cd^{2+} ions (100 μM) and K_2HPO_4 (100 μM) (Fig. 10b and b′).

As Na_2S and K_2HPO_4 can be used for achieving reversibility by respectively removing Cu^{2+} and Al^{3+}/Cd^{2+} ions; logic circuits and truth tables for chemosensors have been constructed (IN 1 = Cu^{2+} and IN 2 = S^{2-} for L1, IN 1 = Al^{3+} or Cd^{2+} and IN 2 = K_2HPO_4 for L2). The threshold emission values were fixed at 150 (for L1), 200 and 100 (for L2) at 418 nm (OUT) for the detection of Cu^{2+}, Al^{3+} and Cd^{2+} ions, respectively (Fig. 9a and 10a). The emission above and below these threshold values were allocated as "ON" and "OFF" for "on" and "off" output signals, respectively.

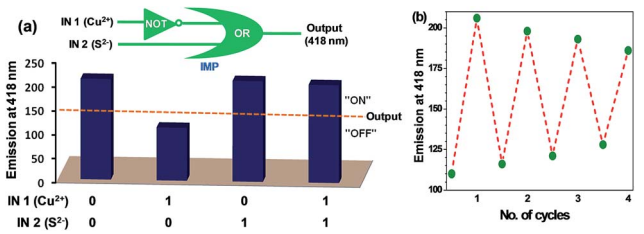

Fig. 9 (a) Emission outputs of L1 at 418 nm in presence of chemical inputs *viz.* IN 1 = Cu^{2+} and IN 2 = S^{2-} (blue bars) and the corresponding two-input combinational logic circuit. (b) Reversibility cycles for L1 (20 μM) at 418 nm upon addition of Cu^{2+} (100 μM) and subsequent regeneration by the addition of Na_2S (200 μM); dotted lines provide guide to eyes.

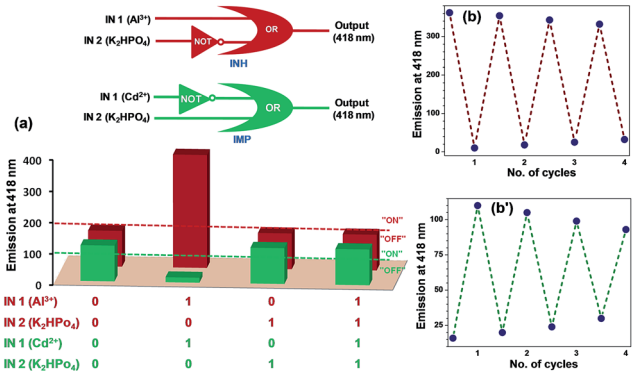

Fig. 10 (a) Emission outputs of L2 at 418 nm in presence of chemical inputs *viz.* IN 1 = Al^{3+} and IN 2 = K_2HPO_4 (red bars); IN 1 = Cd^{2+} and IN 2 = K_2HPO_4 (green bars) and the corresponding two-input combinational logic circuit. (b) and (b′) are reversible cycles for L2 (20 μM) at 418 nm upon addition of Al^{3+} (100 μM) and Cd^{2+} (100 μM), respectively and subsequent regeneration by the addition of K_2HPO_4 (200 μM); dotted lines provide guide to eyes.

Fig. 9a shows the simplest symbolic representation of IMPLICATION (Cu^{2+}) logic gate with two input lines (Cu^{2+} and S^{2-}) of which Cu^{2+} line goes into a single-input NOT gate while outputs from NOT gate and S^{2-} line go into an OR gate. Herein, fluorescence intensity at 418 nm is OR gate output. A similar IMPLICATION (Cd^{2+}) logic gate[38] was observed for Cd^{2+}–K_2HPO_4 system (Fig. 10a, green colored truth table and logic gate). Notably, Al^{3+}–K_2HPO_4 system provided an INHIBIT logic gate[39] wherein Al^{3+} input line goes into a single-input OR gate and K_2HPO_4 input line goes into NOT gate while output from the NOT gate goes into the OR gate (Fig. 10a, red colored truth table and logic gate). In this case, OR gate output is the fluorescence intensity at 418 nm.

Binding modes

Job's method[28,40] of mole fraction suggested 1 : 1 stoichiometry for L1–Cu, L2–Al, L2–Cd and L2–S species (Fig. S20–S22, ESI†). The 1 : 1 stoichiometry was further supported by the Benesi–Hildebrand fitting both from fluorescence as well as UV-Visible spectral titrations (Fig. 3b, 5b, S15 and S19†). Moreover, formation of L1–Cu, L2–Al, L2–Cd and L2–S was also investigated by the UV-Vis titrations (*vide supra*) in which wavelength shift including isosbestic points confirmed the generation of a new species (Fig. 4, 5c and S14, ESI†). We, however, intended to isolate the product(s) from the reaction between different chemosensors to that of metal salts in order to obtain conclusive structural details.

Subsequently, chemosensor L1 was reacted with $CuCl_2$ whereas L2 was treated with $Cd(OAc)_2$ and $Al(NO_3)_3$ salts to obtain the respective product.[41] The FTIR spectrum of the blue-colored L1–Cu complex displayed the disappearance of pyrrole N–H group which was noted at 3326 cm^{-1} in free L1 (Fig. S23†). In addition, $\nu_{C=O}$ stretches for the ester group exhibited negligible shift thus ruling out its involvement in coordination. On the other hand, $\nu_{C=O}$ band of amide group displayed a significant blue shift (from 1602 cm^{-1} in free L1 to 1654 cm^{-1} in L1–Cu) confirming its coordination through the O-amide atom. The

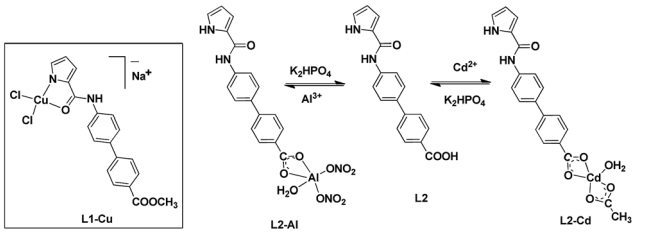

Scheme 2 Chemical drawings of proposed structures of L1–Cu, L2–Al and L2–Cd compounds formed between chemosensors L1/L2 and Cu^{2+}/Al^{3+}/Cd^{2+} ions and the chemical reversibility for the L2–Al and L2–Cd systems.

high-resolution ESI-MS spectrum of L1–Cu displayed molecular ion peak at *m*/*z* 475.9728 attributed to [{L1–H} + Cu^{2+} + $2Cl^-$ + Na^+ + H^+]$^+$ (Fig. S24†). The solution molar conductance of L1–Cu compound displayed non-conducting nature.[42] Collectively, these studies suggest a 1 : 1 stoichiometry between L1 and Cu^{2+} ion forming a L1–Cu compound as displayed in Scheme 2.

Finally, blue colored plate-shaped crystals were obtained by the slow evaporation of a CH_3OH/CH_3CN solution of [L1–Cu] compound. The partial molecular structure however shows a bis-chelated composition, [Cu(L1)$_2$] (Fig. 11).[43] The crystal structure shows a distorted square-planar geometry around the Cu(II) ion wherein two deprotonated pyrrole-N and two neutral O-amide atoms constitute the basal plane around the metal ion. We believe that during the crystallization, a thermodynamically stable product, [Cu(L1)$_2$], was crystallized which is different from the solution-based species [L1–Cu] responsible of sensing of Cu^{2+} ion in solution. Nevertheless, crystal structure of [Cu(L1)$_2$] clearly illustrates the coordination mode of chemosensor L1 and its strong ligating ability.

On the other hand, FTIR spectra of L2–Al and L2–Cd showed two different N–H signals due to the presence of both pyrrole-NH and amide-NH groups thus suggesting protonated form of L2 (Fig. S25 and S26†). In addition, $\nu_{C=O}$ stretches for the carboxylate group exhibited moderate red shift thus suggesting its coordination to the metal ion. The ^{1}H NMR spectrum of L2 in presence of Al^{3+} and Cd^{2+} ions showed disappearance of COO–H signal which was noted at 12.89 ppm in free L2 (Fig. S27†). Therefore, both FTIR and NMR spectral studies confirm the coordination of L2 through the deprotonated carboxylate group in L2–Al and L2–Cd as shown in Scheme 2. The nature of interaction of L2 with Al^{3+} and Cd^{2+} ions was also examined by

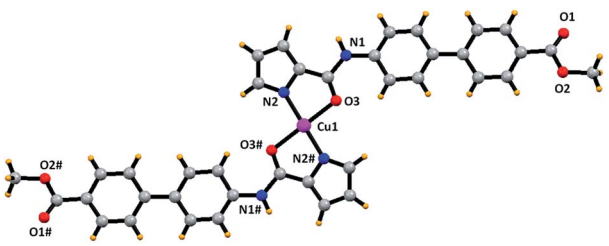

Fig. 11 Ball and stick representation of the partial crystal structure of [Cu(L1)$_2$]. Selected bond distances (Å) and angles (°): Cu1–N2, 1.902; Cu1–O3, 2.014. Selected bond angles (°): O3–Cu1–O3#, 180.0; N2–Cu1–O3, 84.4; N2–Cu1–O3#, 95.6; N2–Cu1–N2, 180.0.

the high-resolution ESI^+ mass spectra. Herein, molecular ion peaks were observed at *m/z* 475.3264 and 531.2752 that were assigned to $[\{L2–H + Al^{3+} + 2NO_3^- + H_2O\} + H^+]^+$ (Fig. S28†) and $[\{L2–H + Cd^{2+} + CH_3COO^- + H_2O\} + Na^+]^+$, respectively (Fig. S29†). The presence of coordinated water in L2–Al and L2–Cd was established by the thermal weight loss (3.4–3.8% for $1H_2O$) in the TGA studies (Fig. S30, ESI†).

Interestingly, when L2–Cd was crystallized from DMSO–CH_3OH, a new compound L2–Cd$^{\#}$ was obtained that was structurally characterized. The asymmetric unit of L2–Cd$^{\#}$ displays two L2, one Cd(II) ion, and two Cd-coordinated DMSO molecules. The crystal structure of L2–Cd$^{\#}$, shown in Fig. 12, exhibits that a Cd(II) ion is coordinated to two O-carboxylate and two O-amide atoms from two different chemosensor L2 in addition to two DMSO molecules. As a result, two chemosensors L2 hold two Cd(II) ions to generate a large metallacycle. Such metallacycles are further extended *via* Cd–O_{amide} bonds to generate a double chain structure. It is suggested that the solution-based species, L2–Cd, slowly reorganizes to form a thermodynamically stable product, L2–Cd$^{\#}$. Importantly, crystal structure of L2–Cd$^{\#}$ proves our assumption that chemosensor L2 coordinates preferentially through its O-carboxylate end and not through pyrrole-N part. Interestingly, crystal structures of $[Cu(L1)_2]$ and L2–Cd$^{\#}$ illustrate that minor changes in a chemosensor (ester *versus* acid) leads to drastic changes in its sensing abilities.

The proton NMR titration of chemosensor L2 with 0–2 equivalents (0, 0.5, 1.0, 1.5 and 2.0) of Na_2S showed changes in the biphenyl ring protons (Fig. S31†). In addition, a new signal was observed at −3.34 ppm that has been assigned to the HS^- species (Fig. S32†).[44] Such an experiment suggests that the interaction of S^{2-} ion with the carboxylic acid group of L2 potentially generates HS^- species and anionic carboxylate group. Importantly, no change in the emission of L1 (having ester group) in presence of S^{2-} ion strongly support the role of free carboxylic acid in its sensing. In the high-resolution ESI-MS spectrum of [L2–S], a peak was observed in the negative mode with *m/z* 341.0679 that corresponded to $[\{L2 + HS^- + H^+\} + H^-]^-$ (Fig. S33†). Collectively, these experiments suggest that the recognition of S^{2-} ion is due to its ability to abstract a proton from COO–H group of the chemosensor L2. Literature has suggested similar mode of interaction and recognition for the sulfide ion.[45]

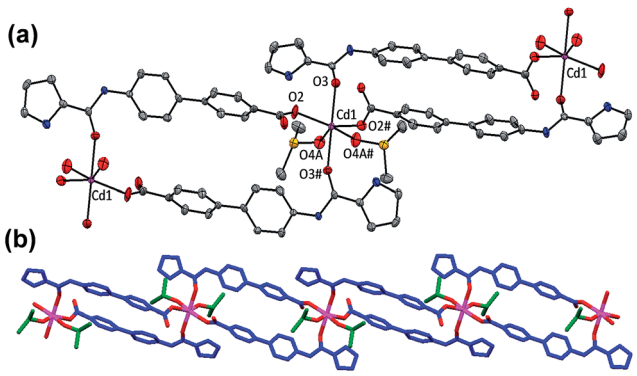

Fig. 12 (a) Crystal structure of L2–Cd$^{\#}$ where thermal ellipsoids are drawn at 30% probability level while hydrogen atoms are omitted for clarity. Selected bond distances (Å): Cd1–O2, 2.206(6); Cd1–O3, 2.278(6); Cd1–O4A, 2.299(14). Selected bond angles (°): O2–Cd1–O2#, 122.6(3); O3–Cd1–O3#, 178.3(4); O4A–Cd1–O4A#, 55.3(8); O2–Cd1–O3, 97.8(2); O2–Cd1–O3#, 83.0(2); O2–Cd1–O4A, 91.7(5); O2–Cd1–O4A#, 145.2(5); O4A–Cd1–O3, 91.6(4); O4A–Cd1–O3#, 87.0(4). (b) An extended view of double chain structure of L2–Cd$^{\#}$.

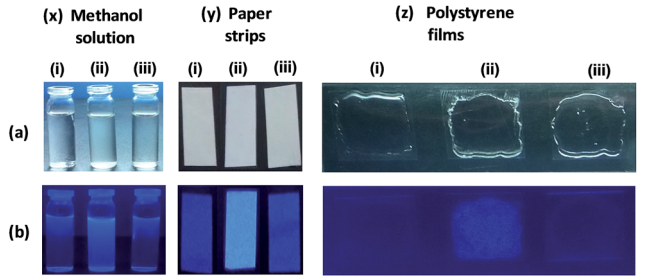

Fig. 13 Detection of Al^{3+} ion in (x) CH_3OH solution (y) paper strips and (z) polystyrene films; (a) and (b) are the images in visible and UV region, respectively. In all cases: (i) displays only L2, (ii) displays L2 in presence of Al^{3+} ion, (iii) displays L2 in presence of Al^{3+} ion and K_2HPO_4. 'y' and 'z' studies have been performed both in H_2O and CH_3OH.

Monitoring of Al^{3+} ion in different systems

In literature, most of the Al-sensors only operate in a solvent, thus, limiting the practical applications.[46] However, straight-forward and cost-effective detection of Al^{3+} ion is important for the practical applications. Therefore, "turn-on" sensing of Al^{3+} ion and its reversibility using K_2HPO_4 provided us an attractive and cost-effective detection opportunity. Towards such a goal, we fabricated filter-paper test strips as well as polystyrene films for the detection of Al^{3+} ion. Fig. 13x exhibits that the presence of Al^{3+} ion in CH_3OH enhances the emission of L2 while addition of K_2HPO_4 quenches the emission. For the monitoring of Al^{3+} ion, filter-paper test strips were prepared by immersing filter-paper strips in a CH_3OH solution of L2 followed by air drying.[47] Such test strips successfully detected Al^{3+} ion by dipping them directly into either CH_3OH or even water solution of Al(III) salt (Fig. 13y). Importantly, if such strips were exposed to an aqueous solution of K_2HPO_4; the original emission of L2 can be retrieved thus providing reversibility. We also attempted to detect Al^{3+} ion using thin polystyrene films. Such thin films were prepared by doping L2 during the synthesis of polystyrene films[28a,48] and demonstrated attractive detection of Al^{3+} ion as well as its reversibility using a solution of K_2HPO_4 (Fig. 13z). Both such detection methods suggest potential monitoring of Al^{3+} ion under environmental as well as industrial conditions.

Conclusions

This report illustrated a simple strategy of developing effective chemosensors for the detection of multiple ions by simply changing the remote functional group. In two related chemosensors, carboxylic acid group was found responsible for the detection of Al^{3+} Cd^{2+}, and S^{2-} ions whereas a pyrrolecarboxamide fragment was needed for the recognition of Cu^{2+} ion.

Utilizing multiple detection abilities of two chemosensors, different logic gates were developed. The "turn on" sensing of Al^{3+} ion helped us in developing filter-paper strips as well as polystyrene films based detection strategies. Facile synthesis and multi-stimuli response offered by the present chemosensors may offer potential detection applications.

Experimental section

The discussion about the Stern–volmer constants (K_{SV}), detection limits, binding constants (K_b) and X-ray crystallography as well as figures for the characterization of L1, L2, L1–Cu, L2–Al, L2–Cd and L2–S can be found in the ESI.†

Materials and physical measurements

The analytical grade commercially available reagents were used without further purifications. Stock solutions (10 mM) of cations and anions were prepared in methanol. HPLC grade solvents were used for the UV-Vis and fluorescence spectral measurements and spectra were recorded with a 1.0 cm path length cuvette at ambient temperature. Elemental analysis data were obtained by the Elementar Analysen Systeme GmbH Vario EL-III instrument. The ^{1}H and ^{13}C NMR spectra recorded with a JEOL 400 MHz instrument. The FTIR spectra (Zn–Se ATR) were recorded with a Perkin-Elmer Spectrum-Two spectrometer. The absorption spectra were recorded with a Perkin-Elmer Lambda–25 spectrophotometer. Fluorescence spectral studies were performed with a Cary Eclipse fluorescence spectrometer. ESI-MS mass spectra were measured with an Agilent Q-TOF LC-MS mass spectrometer.

Synthesis of L1 (methyl 4′-(1*H*-pyrrole-2-carboxamido)-[1,1′-biphenyl]-4-carboxylate)

Pyrrole-2-carboxylic acid (1.0 g, 0.0090 mol) and methyl-4-amino-[1,1-biphenyl]-4-carboxylate (2 g, 0.0090 mol) in 25 mL of pyridine were refluxed for 30 min at 120 °C. $P(OPh)_3$ (3.348 g, 0.0108 mol) was added drop-wise to the aforementioned reaction mixture. The reaction mixture was finally stirred at 80 °C for 12 h. After cooling to room temperature, the reaction mixture was poured into ice-cold water that caused precipitation of the product, which was filtered, washed with water followed by ethanol and dried in vacuum. Yield: 2.2 g (73%). Anal. calc. for $C_{19}H_{16}N_2O_3$: C, 71.24; H, 5.03; N, 8.74. Found: C, 71.31; H, 5.12; N, 8.53. FTIR spectrum (cm^{-1}): 3405 cm^{-1} and 3326 cm^{-1} (N–H). UV/Vis (MeOH): λ_{max} (ε, mol^{-1} cm^{-1}) = 312 (44 240). ESI^+ mass spectrum (MeOH, *m*/*z*): 321.1237 for $[L1 + H]^+$. ^{1}H NMR spectrum (400 MHz, DMSO-d_6): δ = 11.69 (s, 1H), 9.87 (s, 1H), 7.98 (d, J = 8.0 Hz 2H), 7.86 (d, J = 8.3 Hz, 2H), 7.80 (d, J = 8.1 Hz, 2H), 7.71 (d, J = 9.32 Hz, 2H), 7.07 (s, 1H), 6.95 (s, 1H) 6.15 (s, 1H), 3.83 (s, 3H). ^{13}C NMR (DMSO-d_6, 400 MHz): 166.63, 159.74, 144.81, 142.21, 140.38, 133.49, 130.35, 128.37, 127.75, 126.86, 126.48, 123.35, 120.63, 112.10, 109.52, 52.66.

Syntheses of L2 (4′-(1*H*-pyrrole-2-carboxamido)-[1,1′-biphenyl]-4-carboxylic acid)

1 g of L1 was dissolved in 10 mL mixture of THF/water (3 : 1) followed by the addition of a saturated aqueous NaOH solution (5 mL). The said mixture was stirred at room temperature for 8 h. The progress of the reaction was monitored by the thin layer chromatography. After the complete hydrolysis, the reaction mixture was neutralized by the drop-wise addition of 1 N HCl. Subsequently, THF was evaporated under the reduced pressure that caused precipitation of a product. The product was filtered, washed with water and dried under vacuum. Single crystals of L2 were grown by the slow evaporation of a DMSO/H_2O solution. Yield: 0.827 g (93%). Anal. calc. for $C_{18}H_{14}N_2O_3$: C, 70.58; H, 4.61; N, 9.15. Found: C, 70.12; H, 4.52; N, 9.11. FTIR spectrum (cm^{-1}): 3334 cm^{-1} and 3284 cm^{-1} (N–H). UV/Vis (MeOH) λ_{max} (ε, mol^{-1} cm^{-1}) = 307 (41 050). ESI^+ mass spectrum (MeOH, *m*/*z*): 307.1079 for $[L2 + H]^+$. ^{1}H NMR (DMSO-d_6, 400 MHz): δ = 12.89 (s, OH), 11.67 (s, 1H), 9.85 (s, 1H), 7.97 (d, J = 8.3 Hz, 2H), 7.85 (d, J = 8.6 Hz, 2H), 7.70 (d, J = 8.7 Hz, 2H), 7.07 (s, 1H), 6.95 (s, 1H), 6.16 (s, 1H) ^{13}C NMR (DMSO-d_6, 400 MHz): 167.72, 159.73, 144.44, 140.25, 133.75, 130.50, 129.56, 127.71, 126.72, 126.50, 123.32, 120.65, 112.09, 109.51.

Fabrication of filter paper strips and polystyrene films

Strips of Whatman filter paper were dipped in a methanol solution of chemosensor L2 and were air-dried.[47] Test strips coated with L2 were dipped for a few seconds directly into either aqueous or methanolic solution of aluminum nitrate. In another experiment, these test strips were further dipped in an aqueous or methanolic solution of K_2HPO_4. Finally, such test strips were investigated under the visible and ultraviolet light.

A mixture of styrene (1 mL), α,α′-azoisobutyronitrile (AIBN; 1 mg) and L2 in methanol (1 mL) was heated on water bath for 30 min at 80 °C.[28a,48] A few drops of the above solution were placed over glass slide and the slides were air dried to produce the polystyrene film. Such polystyrene films were used for the detection of Al(III) ion by directly dipping them into either aqueous or methanolic solution of aluminum nitrate. To achieve reversibility, such films were dipped into an aqueous or methanolic solution of K_2HPO_4. Such polystyrene films were photographed under the visible and ultraviolet light.

Acknowledgements

RG acknowledges the Council of Scientific and Industrial Research (CSIR), New Delhi and the University of Delhi for the financial support. PK thanks UGC, New Delhi for the award of Dr D. S. Kothari Postdoctoral fellowship. VK thanks UGC, New Delhi for award of junior research fellowship. Authors thank CIF-USIC at this university for the instrumental facilities including X-ray data collection. Authors gratefully acknowledge the crystallographic assistance received by an anonymous referee.

Notes and references

1 (*a*) S. K. Kim and J. L. Sessler, *Acc. Chem. Res.*, 2014, **47**, 2525; (*b*) Y. Huang, F. Li, C. Ye, M. Qin, W. Ran and Y. Song, *Sci. Rep.*, 2015, **5**, 9724; (*c*) M. Ciardi, A. Galan and P. Ballester,

J. Am. Chem. Soc., 2015, **137**, 2047; (*d*) V. Lakshmi and M. Ravikanth, *J. Mater. Chem. C*, 2014, **2**, 5576.

2 (*a*) B. Daly, J. Ling and A. P. de Silva, *Chem. Soc. Rev.*, 2015, **44**, 4203; (*b*) J. Ling, G. Naren, J. Kelly, D. B. Fox and A. P. de Silva, *Chem. Sci.*, 2015, **6**, 4472; (*c*) J. Ling, B. Daly, V. A. D. Silverson and A. P. de Silva, *Chem. Commun.*, 2015, **51**, 8403.

3 (*a*) G. de Ruiter and M. E. van der Boom, *Acc. Chem. Res.*, 2011, **44**, 563; (*b*) M. Kumar, N. Kumar and V. Bhalla, *Chem. Commun.*, 2013, **49**, 877.

4 (*a*) M. Irie, T. Fukaminato, K. Matsuda and S. Kobatake, *Chem. Rev.*, 2014, **114**, 12174; (*b*) X.-J. Jiang and D. K. P. Ng, *Angew. Chem., Int. Ed.*, 2014, **53**, 10481.

5 (*a*) H. Tian, *Angew. Chem., Int. Ed.*, 2010, **49**, 4710; (*b*) A. P. de Silva and S. Uchiyama, *Nat. Nanotechnol.*, 2007, **2**, 399; (*c*) Y. Wu, Y. Xie, Q. Zhang, H. Tian, W. Zhu and A. D. Q. Li, *Angew. Chem., Int. Ed.*, 2014, **53**, 2090.

6 S. Samanta, U. Manna, T. Ray and G. Das, *Dalton Trans.*, 2015, **44**, 18902.

7 (*a*) L. I. Bruijn, T. M. Miller and D. W. Cleveland, *Annu. Rev. Neurosci.*, 2004, **27**, 723; (*b*) B. Wang, W. Xing, Y. Zhao and X. Deng, *Environ. Toxicol. Pharmacol.*, 2010, **29**, 308.

8 C. Vulpe, B. Levinson, S. Whitney, S. Packman and J. Gitschier, *Nat. Genet.*, 1993, **3**, 7.

9 P. C. Bull, G. R. Thomas, J. M. Rommens, J. R. Forbes and D. W. Cox, *Nat. Genet.*, 1993, **5**, 327.

10 (*a*) G. D. Fasman, *Coord. Chem. Rev.*, 1996, **149**, 125; (*b*) T. P. Flaten, *Brain Res. Bull.*, 2001, **55**, 187; (*c*) J. R. Walton, *Neurotoxicology*, 2006, **27**, 385.

11 (*a*) S. Satarug, J. R. Baker, S. Urbenjapol, M. Haswell-Elkins, P. E. B. Reilly, D. J. Williams and M. R. Moore, *Toxicol. Lett.*, 2003, **137**, 65; (*b*) R. A. Goyer, J. Liu and M. P. Waalkes, *BioMetals*, 2004, **17**, 555.

12 (*a*) X. Cao, W. Lin and L. He, *Org. Lett.*, 2011, **13**, 4716; (*b*) R. E. Gosselin, R. P. Smith and H. C. Hodge, Hydrogen sulfide, in *Clinical Toxicology of Commercial Products*, Williams and Wilkins, Baltimore, MD, 5th edn, 1984, pp. III-198–III-202.

13 K. Eto, T. Asada, K. Arima, T. Makifuchi and H. Kimura, *Biochem. Biophys. Res. Commun.*, 2002, **293**, 1485.

14 (*a*) K. P. Carter, A. M. Young and A. E. Palmer, *Chem. Rev.*, 2014, **114**, 4564; (*b*) S. K. Ko, Y. K. Yang, J. Tae and I. Shin, *J. Am. Chem. Soc.*, 2006, **128**, 14150.

15 (*a*) J. Chan, S. C. Dodani and C. J. Chang, *Nature*, 2012, **4**, 973; (*b*) X. L. Zhang, Y. Xiao and X. H. Qian, *Angew. Chem., Int. Ed.*, 2008, **47**, 8025.

16 (*a*) L. Fabrizzi, M. Licchelli, P. Pallavicini, A. Perotti and D. Sacchi, *Angew. Chem., Int. Ed. Engl.*, 1994, **33**, 1975; (*b*) A. Torrado, G. K. Walkup and B. Imperiali, *J. Am. Chem. Soc.*, 1998, **120**, 609; (*c*) Y. Li and C. M. Yang, *Chem. Commun.*, 2003, 2884; (*d*) M. Royzen, Z. Dai and J. W. Canary, *J. Am. Chem. Soc.*, 2005, **127**, 1612; (*e*) Y. Q. Wen, F. Yue, Y. R. Zhong and B. H. Ye, *Inorg. Chem.*, 2007, **46**, 7749; (*f*) S. H. Kim, J. S. Kim, S. M. Park and S.-K. Chang, *Org. Lett.*, 2006, **8**, 371; (*g*) A. Ghorai, J. Mondal, S. Chowdhury and G. K. Patra, *Dalton Trans.*, 2016, **45**, 11540; (*h*) S. Khatua, S. H. Choi, J. Lee, J. O. Huh, Y. Do and D. G. Churchill, *Inorg. Chem.*, 2009, **48**, 1799; (*i*) A. Paul, S. Anbu, G. Sharma, M. L. Kuznetsov, M. F. C. G. da Silva, B. Koch and A. J. L. Pombeiro, *Dalton Trans.*, 2015, **44**, 16953.

17 (*a*) Q. Wu and E. V. Anslyn, *J. Am. Chem. Soc.*, 2004, **126**, 14682; (*b*) Z. C. Wen, R. H. Yang, H. He and Y. B. Jiang, *Chem. Commun.*, 2006, 106; (*c*) L. Zheng, E. W. Miller, A. Pralle, E. Y. Isacoff and C. J. Chang, *J. Am. Chem. Soc.*, 2006, **128**, 10; (*d*) Z. C. Xu, Y. Xiao, X. H. Qian, J. N. Cui and D. W. Cui, *Org. Lett.*, 2005, **7**, 889; (*e*) J. J. Lee, Y. W. Choi, G. R. You, S. Y. Lee and C. Kim, *Dalton Trans.*, 2015, **44**, 13305; (*f*) G. K. Li, Z. Xu, X. C. F. Chen and Z. T. Huang, *Chem. Commun.*, 2008, 1774; (*g*) S. Khatua, S. H. Choi, J. Lee, J. O. Huh, Y. Do and D. G. Churchill, *Inorg. Chem.*, 2009, **48**, 1799; (*h*) G. R. You, G. J. Park, J. J. Lee and C. Kim, *Dalton Trans.*, 2015, **44**, 9120; (*i*) S. H. Choi, K. Pang, K. Kim and D. G. Churchill, *Inorg. Chem.*, 2007, **46**, 10564; (*j*) M. Li, X.-J. Jiang, H.-H. Wu, H.-L. Lu, H.-Y. Li, H. Xu, S.-Q. Zang and T. C. W. Mak, *Dalton Trans.*, 2015, **44**, 17326.

18 (*a*) S. Goswami, K. Aich, S. Das, A. K. Das, D. Sarkar, S. Panja, T. K. Mondal and S. Mukhopadhyay, *Chem. Commun.*, 2013, **49**, 10739; (*b*) A. Sahana, A. Banerjee, S. Lohar, B. Sarkar, S. K. Mukhopadhyay and D. Das, *Inorg. Chem.*, 2013, **52**, 3627; (*c*) C. Liang, W. Bu, C. Li, G. Men, M. Deng, Y. Jiangyao, H. Sun and S. Jiang, *Dalton Trans.*, 2015, **44**, 11352; (*d*) S. Das, M. Dutta and D. Das, *Anal. Methods*, 2013, **5**, 6262; (*e*) D. Maity and T. Govindaraju, *Chem. Commun.*, 2010, **46**, 4499; (*f*) K. K. Upadhyay and A. Kumar, *Org. Biomol. Chem.*, 2010, **8**, 4892; (*g*) C.-H. Chen, D.-J. Liao, C.-F. Wan and A.-T. Wu, *Analyst*, 2013, **138**, 2527; (*h*) J. F. Wang and Y. Pang, *RSC Adv.*, 2014, **4**, 5845; (*i*) Y.-W. Liu, C.-H. Chen and A.-T. Wu, *Analyst*, 2012, **137**, 5201; (*j*) S. Tao, X. Li, C. Wang and C. Meng, *ChemistrySelect*, 2016, **1**, 3208.

19 (*a*) X. Peng, J. Du, J. Fan, J. Wang, Y. Wu, J. Zhao, S. Sun and T. Xu, *J. Am. Chem. Soc.*, 2007, **129**, 1500; (*b*) R. T. Bronson, D. J. Michaelis, R. D. Lamb, G. A. Husseini, P. B. Farnsworth, M. R. Linford, R. M. Izatt, J. S. Bradshaw and P. B. Savage, *Org. Lett.*, 2005, **7**, 1105; (*c*) T. Gunnlaugsson, T. C. Lee and R. Parke, *Org. Lett.*, 2003, **5**, 4065; (*d*) W. Liu, L. Xu, R. Sheng, P. Wang, H. Li and S. Wu, *Org. Lett.*, 2007, **9**, 3829; (*e*) T. Cheng, Y. Xu, S. Zhang, W. Zhu, X. Qian and L. Duan, *J. Am. Chem. Soc.*, 2008, **130**, 16160; (*f*) X.-L. Tang, X.-H. Peng, W. Dou, J. Mao, J.-R. Zheng, W.-W. Qin, W.-S. Liu, J. Chang and X.-J. Yao, *Org. Lett.*, 2008, **10**, 3653; (*g*) Z. Xu, G. Li, Y.-Y. Ren, H. Huang, X. Wen, Q. Xu, X. Fan, Z. Huang, J. Huang and L. Xu, *Dalton Trans.*, 2016, **45**, 12087; (*h*) C. Lu, Z. Xu, J. Cui, R. Zhang and X. Qian, *J. Org. Chem.*, 2007, **72**, 3554; (*i*) A. Visscher, S. Bachmann, C. Schnegelsberg, T. Teuteberg, R. A. Matac and D. Stalke, *Dalton Trans.*, 2016, **45**, 5689; (*j*) H.-L. Lu, W.-K. Wang, X.-X. Tan, X.-F. Luo, M.-L. Zhang, M. Zhang and S.-Q. Zang, *Dalton Trans.*, 2016, **45**, 8174.

20 (*a*) X. Cao, W. Lin and L. He, *Org. Lett.*, 2011, **13**, 4716; (*b*) M. G. Choi, S. Cha, H. Lee, H. L. Jeon and S.-K. Chang,

Chem. Commun., 2009, 7390; (*c*) L. Zhang, X. Lou, Y. Yu, J. Qin and Z. Li, *Macromolecules*, 2011, **44**, 5186; (*d*) K. M. Vengaian, C. D. Britto, K. Sekar, G. Sivaraman and S. Singaravadivel, *Sens. Actuators, B*, 2016, **235**, 232.

21 (*a*) D. P. Bhopate, P. G. Mahajan, K. M. Garadkar, G. B. Kolekar and S. R. Patil, *New J. Chem.*, 2015, **39**, 7086; (*b*) C. R. Liu, J. Pan, S. Li, Y. Zhao, L. Y. Wu, C. E. Berkman, A. R. Whorton and M. Xian, *Angew. Chem., Int. Ed.*, 2011, **50**, 10327; (*c*) K. Sasakura, K. Hanaoka, N. Shibuya, Y. Mikami, Y. Kimura, T. Koma, T. Ueno, T. Ter, H. Kimura and T. Nagano, *J. Am. Chem. Soc.*, 2011, **133**, 18003.

22 H. Komatsu, T. Miki, D. Citterio, T. Kubota, Y. Shindo, Y. Kitamura, K. Oka and K. Suzuki, *J. Am. Chem. Soc.*, 2005, **127**, 10798.

23 (*a*) Z. Zhang, Y. Zou and C. Deng, *RSC Adv.*, 2017, **7**, 14742; (*b*) S. Qu, C. Zheng, G. Liao, C. Fan, G. Liu and S. Pu, *RSC Adv.*, 2017, **7**, 9833.

24 (*a*) A. Barba-Bon, A. M. Costero, S. Gil, M. Parra, J. Soto, R. Martınez-Manez and F. Sancenon, *Chem. Commun.*, 2012, **48**, 3000; (*b*) C. Marin-Hernandez, L. E. Santos-Figueroa, M. E. Moragues, M. M. M. Raposo, R. M. F. Batista, S. P. G. Costa, T. Pardo, R. Martinez-Manez and F. Sancenon, *J. Org. Chem.*, 2014, **79**, 10752; (*c*) M. L. Presti, S. E. Sayed, R. Martınez-Manez, A. M. Costero, S. Gil, M. Parra and F. Sancenon, *New J. Chem.*, 2016, **40**, 9042; (*d*) K. Chen, J. W. Bats and M. Schmittel, *Inorg. Chem.*, 2013, **52**, 12863.

25 C. Caltagirone, V. Lippolis, F. Isaia, A. Garau, M. A. Scorciapino, A. Casula, R. Martinez-Manez, F. Sancenon, C. Santi, M. Kubicki, A. Owczarzak and A. Llopis-Lorente, *Chem. Commun.*, 2017, **53**, 3729.

26 (*a*) K. Chen and M. Schmittel, *Anal. Bioanal. Chem.*, 2016, **408**, 7077; (*b*) K. Chen and M. Schmittel, *Chem. Commun.*, 2014, **50**, 5756; (*c*) K. Chen, Q. Shu and M. Schmittel, *Chem. Soc. Rev.*, 2015, **44**, 136; (*d*) K. Chen and M. Schmittel, *Analyst*, 2013, **138**, 6742; (*e*) Q. Shu, L. Birlenbach and M. Schmittel, *Inorg. Chem.*, 2012, **51**, 13123.

27 G. W. Bates, P. A. Gale and M. E. Light, *Chem. Commun.*, 2007, 2121.

28 (*a*) D. Bansal and R. Gupta, *Dalton Trans.*, 2016, **45**, 502; (*b*) D. Bansal, G. Kumar, G. Hundal and R. Gupta, *Dalton Trans.*, 2014, **43**, 14865; (*c*) P. Kumar, V. Kumar and R. Gupta, *RSC Adv.*, 2015, **5**, 97874.

29 S. Paul, S. Goswami and C. D. Mukhopadhyay, *New J. Chem.*, 2015, **39**, 8940.

30 H. A. Benesi and J. H. Hildebrand, *J. Am. Chem. Soc.*, 1949, **71**, 2703.

31 S. Goswami, K. Aich, A. K. das, A. Manna and S. Halder, *Analyst*, 2013, **138**, 1909.

32 C. Fan, S. Wang, J. W. Hong, G. C. Bazan, K. W. Plaxco and A. J. Heeger, *Proc. Natl. Acad. Sci. U. S. A.*, 2003, **100**, 6297.

33 (*a*) D. Margulies, C. E. Felder, G. Melman and A. Shanzer, *J. Am. Chem. Soc.*, 2007, **129**, 347; (*b*) L. Feng, Z. Lyu, A. Offenhausser and D. Mayer, *Angew. Chem., Int. Ed.*, 2015, **54**, 7693; (*c*) J. Andreasson and U. Pischel, *Chem. Soc. Rev.*, 2015, **44**, 1053.

34 (*a*) J. Andreasson and U. Pischel, *Chem. Soc. Rev.*, 2015, **44**, 1053; (*b*) J. Andreasson and U. Pischel, *Chem. Soc. Rev.*, 2010, **39**, 174; (*c*) A. P. de Silva, *Molecular Logic-based Computation*, The Royal Society of Chemistry, Cambridge, 2013.

35 (*a*) D. C. Magri and A. P. de Silva, *New J. Chem.*, 2010, **34**, 476; (*b*) A. P. De Silva and S. Uchiyama, *Nat. Nanotechnol.*, 2007, **2**, 399; (*c*) X. J. Zhao and C. Z. Huang, *Analyst*, 2010, **135**, 2853.

36 A. Visscher, S. Bachmann, C. Schnegelsberg, T. Teuteberg, R. A. Matac and D. Stalke, *Dalton Trans.*, 2016, **45**, 5689.

37 (*a*) M. Sun, H. Yu, H. Li, H. Xu, D. Huang and S. Wang, *Inorg. Chem.*, 2015, **54**, 3766; (*b*) Y. F. Zhu, D. H. Fan and W. Z. Shen, *J. Phys. Chem. C*, 2008, **112**, 10402.

38 R.-R. Gao, S. Shi, Y. Zhu, H.-L. Huang and T.-M. Yao, *Chem. Sci.*, 2016, **7**, 1853.

39 S. Goswami, A. Manna, S. Paul, K. Aich, A. K. Das and S. Chakraborty, *Dalton Trans.*, 2013, **42**, 8078.

40 A. Senthilvelan, I. Ho, K. Chang, G. Lee, Y. Liu and W. Chung, *Chem.–Eur. J.*, 2009, **15**, 6152.

41 In each case, chemosensor L1 or L2 was reacted with the respective metal salt in a 1 : 1 stoichiometry in CH_3OH. In all cases, reaction led to a clear solution from which the product was isolated after the removal of solvent under the reduced pressure. Such products were further purified by the forced precipitation from a CH_3OH solution using excess diethyl ether.

42 G. W. Geary, *Coord. Chem. Rev.*, 1971, **7**, 81.

43 Complex $[Cu(L1)_2]$ always produced poorly-diffracting thin plate-like crystals and one such effort resulted in data collection and structure solution. However, poor structure convergence only allowed partial structure. Crystal data: cell = monoclinic; space group = $P2_1/n$; $a = 5.0716(19)$, $b = 18.084(6)$, $c = 17.170(5)$; $\alpha = \gamma = 90$, $\beta = 90.06(3)$; $V = 1574.7(9)$; $Z = 2$.

44 M. D. Hartle, D. J. Meininger, L. N. Zakharow, Z. J. Tonzetich and M. D. Pluth, *Dalton Trans.*, 2015, **44**, 19782.

45 (*a*) Y. Qian, J. Karpus, O. Kabil, S.-Y. Zhang, H.-L. Zhu, R. Banerjee, J. Zhao and C. He, *Nat. Commun.*, 2011, **2**, 495; (*b*) T. D. Ashton, K. A. Jolliffeb and F. M. Pfeffer, *Chem. Soc. Rev.*, 2015, **44**, 4547.

46 S. Paul, A. Manna and S. Goswami, *Dalton Trans.*, 2015, **44**, 11805.

47 M. Wang, X. Liu, H. Lu, H. Wang and Z. Qin, *ACS Appl. Mater. Interfaces*, 2015, **7**, 1284.

48 P. Kumar, V. Kumar and R. Gupta, *RSC Adv.*, 2017, **7**, 7734.